ELSEVIER

Carbohydrate Polymers 49 (2002) 439–448

Carbohydrate Polymers

www.elsevier.com/locate/carbpol

Spherulitic crystallization of gelatinized maize starch and its fractions

Tor S. Nordmark, Gregory R. Ziegler*

Department of Food Science, The Pennsylvania State University, 116 Borland Laboratory, University Park, PA 16802, USA

Received 15 June 2001; revised 11 October 2001; accepted 20 October 2001

Abstract

Binary systems of polymers often display spherulitic morphologies after cooling from the melt, but these phenomena have rarely been reported among food polymers of native-size. Here we report the observation of spherulitic and other morphologies in gelatinized maize starch. The morphology could be manipulated by choosing polymer compositions and kinetic regimes. Spherulites (~10 μm diameter) formed from gelatinized high-amylose maize starches and purified amylose at cooling rates of order of magnitude 100 °C/min. They were more numerous and exhibited a higher melting point the greater the ratio of amylose to amylopectin. Rapid cooling rates (150–500 °C/min) resulted in a more even distribution of smaller spherulites. Very rapid (liquid nitrogen quench) or slow (0.1–1 °C/min) cooling rates resulted in mixed morphology, as did addition of 15 or 60% (w/w) sucrose to a 10% (w/w) dispersion of high-amylose starch (HAS). Spherulites were observed in aqueous suspensions of high-amylose maize starch between 5 and 30% (w/w). Lower starch concentrations resulted in a broader size distribution and spherulites of more distinct shape. WAXS patterns of B-type were observed. Negatively birefringent spherulites predominated, but positive spherulites were found. The spherulite melting range overlapped with that for amylose–lipid complex. Evidence indicated that micro-phase separation takes place when a holding period at 95 °C follows gelatinization at 180 °C. Despite the high maximum temperature of treatment (180 °C) there was evidence for a memory effect in samples of 30% HAS. Spherulite morphology closely resembled that of native starch granules in very early stages of development. © 2002 Elsevier Science Ltd. All rights reserved.

Keywords: High-amylose maize starch; Crystallization; Spherulite; Granule formation

1. Introduction

Crystallization of polymers may result in a variety of morphologies, e.g. lamellae, fibrils, spherulites, or axialites (Sharples, 1966). Generally one form or other predominates under any set of thermodynamic and kinetic conditions. Spherulites are birefringent entities, radial in symmetry, which form at a high degree of under-cooling (deep quenches) in a medium of high viscosity and in the presence of some impurity that can be rejected from the growing crystal front. In synthetic polymers, branched, atactic, or low molecular weight components, which crystallize less readily than the bulk polymer, serve as this impurity (Sharples, 1966). Spherulites exhibit a 'Maltese cross' when viewed by transmission optical microscopy between crossed polarizers, and are the basic morphology of synthetic polymers crystallized from the melt or concentrated solutions free from stress (Haudin, 1986), but are rare among biopolymers. Recently, both positive and negative cellulose spherulites have been obtained via enzymatic polymerization of β-cellobiosyl fluoride by cellulase (Kobayashi et al., 2000). Negative spherulites approximately 10 μm in diameter predominated. Crystal lamellae, the thickness of which (10 nm) roughly corresponded to the length of the cellulose chains (degree of polymerization 16) were found to radiate out from the center. Spherulite formation required the presence of the quartz cell surface (Kobayashi et al., 2000).

Starch spherocrystals (i.e. spherulites) up to a diameter of 75 μm containing a 'hilum' of radially-oriented fibrous crystals have been grown from glucose-1-phosphate in the presence of phosphorylase (Sandstedt, 1965). Ring, Miles, Morris, Turner, and Colonna (1987) precipitated spherulites 10–15 μm in diameter by cooling aqueous solutions of 5–20 wt% amylose, average degree of polymerization 22, to 2 °C. The wetted precipitate gave very sharp powder diffraction patterns of the B type, and an endothermic peak was observed by differential scanning calorimetry at 74 °C (Ring et al., 1987). Spherulites of low molecular weight amylose exhibiting the A-type diffraction pattern have been precipitated from ethanolic solutions (Helbert, Chanzy, Planchot, Buleon, & Colonna, 1993; Ring et al., 1987). Electron microscopy and electron diffraction analyzes revealed a radial orientation of the helical axis, confirming the positive nature of the birefringence (Helbert et al., 1993). Godet,

* Corresponding author. Tel.: +1-814-863-2960; fax: +1-814-863-6132.
E-mail address: grz1@psu.edu (G.R. Ziegler).

0144-8617/02/$ - see front matter © 2002 Elsevier Science Ltd. All rights reserved.
PII: S0144-8617(01)00353-8

Bouchet, Colonna, Gallant, and Buleon (1996) observed spherocrystals of amylose (DP 80)–fatty acid complexes displaying a core and a cortex composed of lamella oriented in the radial direction.

Davies, Miller, and Proctor (1980) observed the formation of spherocrystallites when gelatinized (150 °C) commercial maize starch, high-amylose maize starch or rice starch were held at temperatures greater than 75 °C, a phenomenon they termed high-temperature retrogradation. Generally, these particles did not form at temperatures below 70 or above 95 °C. These regular spherical particles, 15–40 μm in diameter, comprised fibrils of 10–20 nm wide, 200–400 nm long, separated by 10–20 nm. The authors postulated that the particles were formed via crystallization of amylose–lipid complexes, but provided no direct evidence, e.g. XRD patterns.

The gelatinized starch system is a pseudo-binary blend of amylose and amylopectin that is, for the most part, not in thermodynamic equilibrium. Crystal morphology in polymers is determined primarily by kinetic factors rather than characteristics of an equilibrium state (Bassett, 1981). Cho, Li, and Choi (1999) observed either co-crystallization or phase separation in polypropylene and maleated polypropylene blends depending on the thermal treatment. Phase separation was observed when the cooling rate was very low or the crystallization temperature was high. Kalichevsky and Ring (1987) demonstrated phase separation between pea amylose and waxy maize amylopectin in aqueous dispersions at 80 °C. The threshold of separation occurred at 2% amylose/1.5% amylopectin. Yuryev, Nemirovakaya, and Maslova (1995) concluded that amylose–amylopectin blends were biphasic when dispersed in water at concentrations up to 30% (w/w), and Leloup, Colonna, and Buleon (1991) found evidence for phase inversion in potato amylose/waxy maize amylopectin blends at an amylose:amylopectin ratio of 0.43 with 8% total polymer. Phase separation can occur both in the swollen granule and in molecular dispersions, and is generally enhanced at higher temperatures, e.g. 120 °C (Hermansson, Kidman, & Svegmark, 1995). The study of starch polymer association is complicated by the overlap of the temperature ranges over which the potentially inter-related phenomena of crystallization, amylose–lipid complexation, phase separation and gelation occur on cooling of gelatinized starch.

In this paper, we report the observation of spherulites from the crystallization of native-size maize starch polymers and the general conditions for their formation, and discuss the implications of this research relevant to the biosynthesis of the starch granule.

2. Materials and methods

2.1. Materials

Granular high-amylose, *ae* 50 and 70, maize starch (Hylon V and VII), normal maize starch (Melojel) and waxy maize starch (WMS) (Amioca) were obtained from National Starch and Chemical (Bridgewater, NJ). Non-granular, lipid-free, dispersed and dried starch (DDS) was prepared from *ae* 70 following the protocol of Klucinec (1997). High-purity amylose (AM), >98%, and amylopectin (AP), >99%, were prepared from *ae* 70 and WMS, respectively, following the procedure of Takeda, Hizukuri, and Juliano (1986) as modified by Klucinec and Thompson (1996). DDS and a blend of amylose and amylopectin in the same proportions present in native *ae* 70 served as model systems to aid in interpretation of data, especially the effect of lipid and residual granular order. The total polymer contents of *ae* 50 and 70 were previously determined (Klucinec, personal communication) to be 87% (w/w), and that of all other preparations were assumed to be 90% (w/w). Water was treated in a NANOpure water purification system (Barnstead/Thermolyne, Dubuque, IO).

2.2. Differential scanning calorimetry

A DSC-7 operated with Pyris software for Windows v3.52 (Perkin–Elmer Instruments, Norwalk, CT) was used for thermal analysis. Sealed stainless steel DSC pans (60 μl) were purchased from Perkin–Elmer Instruments (Norwalk, CT). A starch concentration of 30% (w/w) in water was used unless otherwise specified. Samples were prepared by gentle but thorough mixing in DSC pans and stored in closed pans at 20 °C for at least one day to facilitate moisture equilibration (De Meuter, Amelrijckx, Rahier, & Van Mele, 1999; Hoover, 1995). Samples were heated to 180 °C at 10 °C/min before a particular cooling regime was applied. The choice of maximum temperature is in agreement with an extrapolated dissolution temperature for B-type crystalline amylose of 147 °C at 80% water content (Moates, Noel, Parker, & Ring, 1997). De Meuter et al. (1999) considered heating to 170 °C is sufficient to ensure amorphous nature in starch samples. No significant weight loss was observed. Treated samples were subsequently either scanned in the DSC at 10 °C/min, or the pans were opened and used for optical microscopy, SEM, or X-ray diffractometry after a storage period as applicable. Samples were carefully collected from the pans with a blunt end spatula. Experiments were conducted at least in duplicate.

2.3. Microscopy

A Nikon Diaphot 300 inverted microscope (Nikon, Melville, NY) and a liquid-cooled CCD camera of type Nu 200 (Photometrics, Tucson, AZ) were used for conventional and polarized light microscopy in differential interference contrast mode. The image processing software was IPLab Spectrum H-SU2, v2.5.7 (Signal Analytics, Vienna, VA). An Olympus BH-2 microscope (Olympus America, Melville, NJ) equipped with a Mettler FP 82 hot stage (Mettler Instrument, Highstown, NJ) was used for thermal ramp studies. Samples were scanned from 60 to 115 °C at a

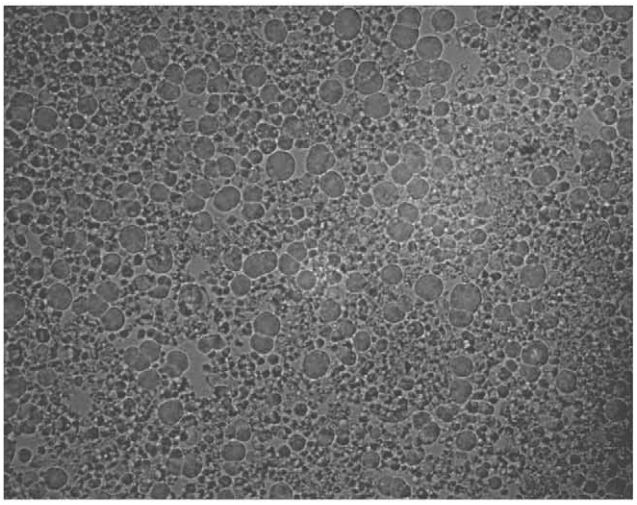

(a)

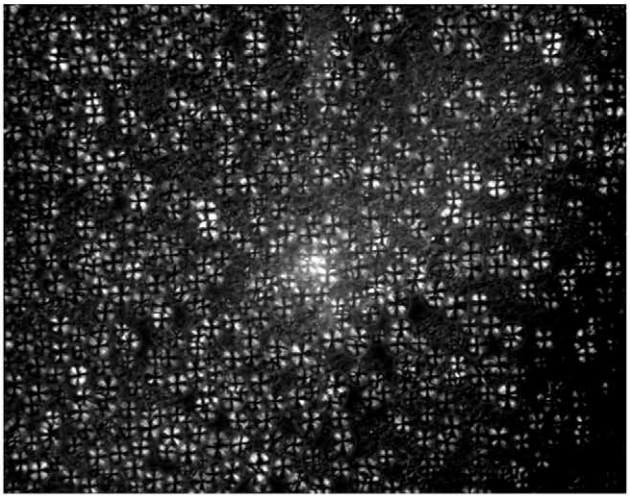

(b)

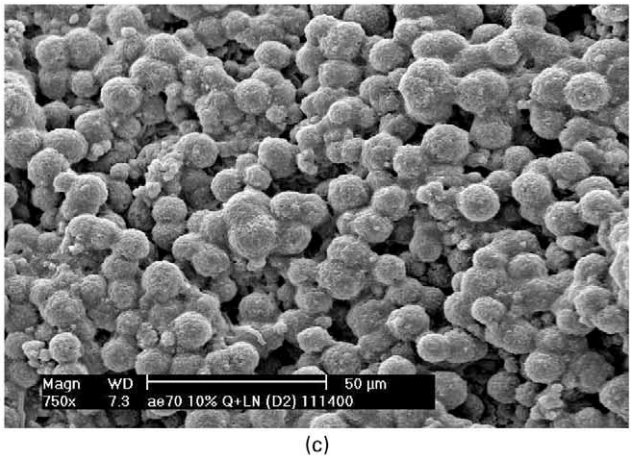

(c)

Fig. 1. Morphology of gelatinized HAS (*ae* 70 HAS) dispersion produced at fast (10 °C/min) cooling rate: (A) transmission light microscopy (image size $285 \times 360\ \mu m^2$), (B) polarized light microscopy (image size $285 \times 360\ \mu m^2$), and (C) scanning electron microscopy.

rate of 5 °C/min. Cover glasses were sealed to microscope slides using either Cytoseal-60 (Stephens Scientific, Riverdale, NJ) or Loctite 369 (Loctite, Rocky Hill, CT). Microscopy was performed at ambient temperature unless otherwise noted.

A Philips XL20 (FEI/Philips Electron Optics, Hillsboro, OR) scanning electron microscope was used for SEM studies. An ultrasonic bath (model 1200, Branson Cleaning Equipment, Shelton, CT) and a gold sputtering device (Iumme Technics, Alexandria, VA) were employed in sample preparation. Samples were initially prepared in the DSC as described earlier. The content of the DSC pan was removed by adding filtered (0.45 μm) water using a micropipette. The starch–water suspension, which was kept at 0 °C in the case of amylopectin, was stirred magnetically at moderate speed for 10 min and then treated, unless otherwise specified, in a low power (80 W) ultrasonic bath for 5 min. The suspension was then filtered through a 0.45 μm polysulfone membrane, air dried at ambient temperature (or 5 °C in the case of amylopectin), and stored in a closed container. The sample was sputter coated in a low-pressure argon atmosphere for ~1 min to obtain a gold layer of ~10 nm thickness. Both an untreated membrane and a membrane that had been subjected to all preparation steps described earlier were viewed in the electron microscope. In both cases, the membrane surface contained numerous equally sized (<1 μm), smooth, droplet-shaped polysulfone phases connected to the mesh that were easily distinguishable from starchy material.

Selected semi-crystalline starchy materials were subjected to polarized light microscopy using the technique of wave retardation for the determination of the orientation of their axes of highest refractive index (Haudin, 1986). This orientation is generally assumed to coincide with the average orientation of the long chain axis of the polymer. The spectrum of the light source was, after filtering, approximately equal to a daylight spectrum. Retardation (about 565 nm path difference) was accomplished by inserting a (first order red) full wave plate of crystalline gypsum at an angle 45° relative to the polarization axes. The positioning of the retardation colors (blue and yellow) in relation to the refractive indicatrix of the retardation plate allowed the determination of whether the retardation provided by the plate was increased or decreased by the presence of oriented polymer chains in different regions (quadrants) of the spherulite. Thereby the orientation of the long chain axes within these regions could be determined.

2.4. X-ray diffraction

A Philips X'pert Multi-purpose X-ray diffractometer (Philips Analytical, Natick, MA) equipped with a copper anode and a 0.154 nm ($Cu\ K_\alpha$) monochromator operated at 40 V/40 mA was used for comparative crystallography. Scan rates between 0.48 and 2.4°/min and sample size between 20 and 200 mg were employed in the range 2θ

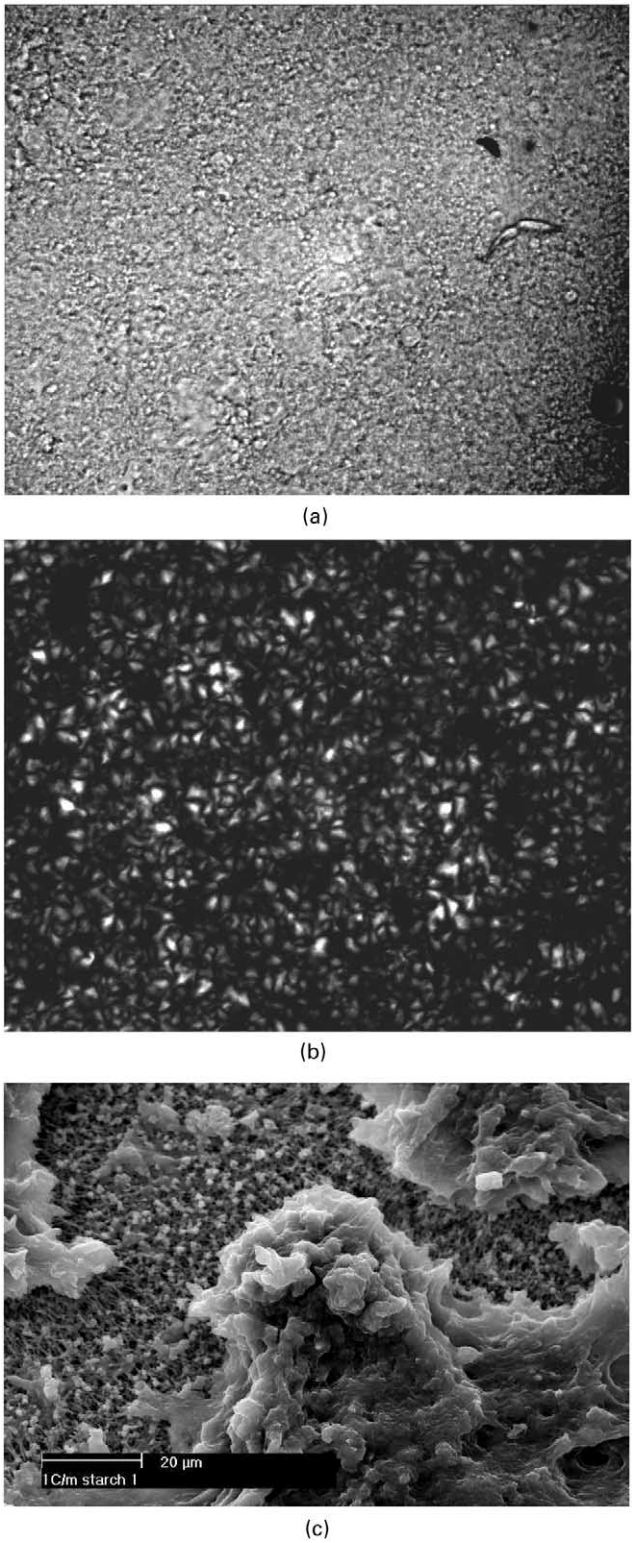

Fig. 2. Morphology of gelatinized HAS (*ae* 70 HAS) dispersion produced at slow (1 °C/min) cooling rate: (A) transmission light microscopy (image size $285 \times 360\ \mu m^2$), (B) polarized light microscopy (image size $285 \times 360\ \mu m^2$), and (C) scanning electron microscopy.

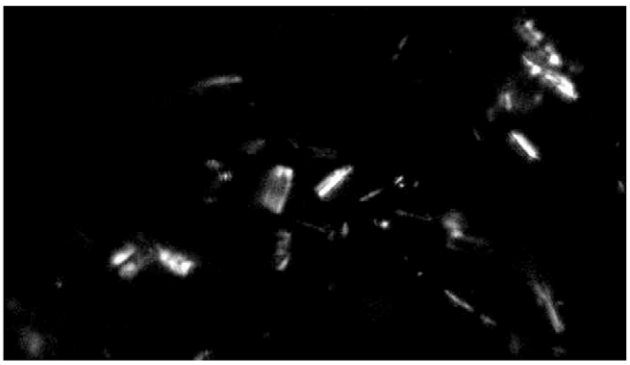

Fig. 3. Optically-active microfibril produced from gelatinized *ae* 70 HAS at slow (0.1 °C/min) cooling rate (image size $100 \times 180\ \mu m^2$).

from 2 to 50°. Samples for X-ray diffractometry were prepared in the DSC by heating to 180 °C followed by cooling, either fast or slow, to 10 °C as described earlier. The contents of several pans were carefully pooled together to provide a satisfactory detector response and stored in small closed vials at 5 °C until used. Samples were scanned in the wet state, nominally 70 % (w/w) moisture.

3. Results and discussion

3.1. Influence of cooling rate on crystal morphology

Aqueous samples of 10% *ae* 70 high-amylose starch (HAS) were cooled in the DSC from 180 to 10 °C at four cooling rates: 0.1, 1, 10, and 500 °C/min. For the two slower cooling rates, samples were first quenched to 120 °C before carrying on the prescribed cooling rate to avoid polymer degradation by exposure to long times at higher temperatures. The samples were then observed after 2 days storage at 20 °C by microscopy and DSC. Very rapid cooling was accomplished by transferring a DSC pan, first heated to 180 °C in an ordinary laboratory oven, within 2–3 s into a cryoflask with enough liquid nitrogen (−195 °C) to cover the pan for few minutes.

Numerous circular, birefringent entities exhibiting a Maltese cross (i.e. spherulites) were observed in rapidly-cooled (10 or 500 °C/min) gelatinized *ae* 70 HAS (Fig. 1). Spherulite diameter was somewhat dependent on cooling rate, averaging between 10 and 15 μm. Spherulites of varying sizes were rarely found at cooling rates of 0.1 and 1.0 °C/min. Instead, rod-shaped or irregular fuzzy clusters (Fig. 2) appeared that were optically active and often bright, but did not display the Maltese cross typical of spherulites. Optically active microfibrils similar to those typical of cellulose (Battista, 1975; Sharples, 1966) were also observed at slow cooling rates (Fig. 3). Maxfield and Mandelkern (1977) observed rod structures in low molecular weight linear polyethylene upon crystallization at high-temperature (shallow quenches) and identified them as axialites. Extremely rapid cooling by immersion in liquid

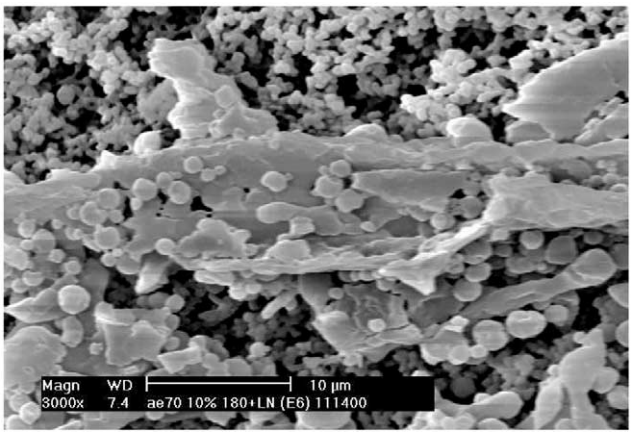

Fig. 4. Morphology produced at extremely rapid cooling rate attained by immersion of gelatinized *ae* 70 HAS in liquid nitrogen.

nitrogen resulted in a mixed morphology containing many small (1–3 μm diameter) spherical particles and much larger sheets or lamellae (Fig. 4). Extremely fast or slow cooling rates do not allow for spherulite formation due to limited time for diffusion and reorganization of components in the first case and a thermodynamically favored near-equilibrium rearrangement (spherulites are considered to be metastable) in the second case.

Fig. 5 presents the DSC thermograms obtained on reheating after 2 days of storage at 20 °C. For samples prepared at faster cooling rates (10 and 500 °C/min), a broad endotherm with a peak temperature in the range 60–100 °C and an enthalpy of ~8 J/g was observed. A small endotherm ($\Delta H \sim 3$ J/g) with a peak temperature of 160–180 °C was also present. At the slower cooling rates (0.1 and 1.0 °C/min), the high-temperature endotherm grew at the expense of the low-temperature peak, attaining a melting enthalpy of 25–30 J/g. At 0.1 °C/min, the low-temperature peak appeared at 108 °C. For rapidly-cooled samples viewed using polarized light microscopy, Maltese crosses were lost on heating to 95–100 °C, suggesting that the endotherm observed just below this range by DSC was the melting of spherulites, since birefringence may persist after the melting endotherm due to orientation of polymer chains despite the loss of crystallinity (Sharples, 1966). We are suggesting that the high-temperature endotherm corresponds to higher melting crystallites, perhaps revealed as the rod-shaped, birefringent entities.

Wide-angle X-ray diffraction of pooled samples of both *ae* 70 HAS and DDS exhibiting predominantly spherulitic morphology (prepared at cooling rates of 10 and 500 °C/min) revealed a weak B-type pattern, with some V_h-type likely present (Fig. 6). Slow cooling rates (0.1 and 1.0 °C/min) resulted in even weaker B-type patterns. This is consistent with the B-type pattern of the native HAS granule (Cheetham & Tao, 1998; Richardson, Jeffcoat, & Shi, 2000) and for amylose gels (Leloup, Colonna, Ring, Roberts, & Wells, 1992).

The spherulites obtained were for the most part negatively birefringent, suggesting that the main axes of the polymer chains were oriented tangentially to the radial direction (Haudin, 1986). Many starch granules and A-type spherulites from short-chain (DP 15) potato amylose display positive birefringence (Helbert et al., 1993), implying that the main axes of the polymer chain are oriented in a radial direction (Haudin, 1986). However, different crystals obtained from the same polymeric material have been observed to possess both positive and negative birefringence depending on the crystallization path (Kobayashi et al., 2000; Ring et al., 1987). Some positive spherulites were observed in samples that included a holding period at 95 °C during the cooling ramp (see next).

Spherulites were observed to form from gelatinized *ae* 70 HAS in the concentration range 5–30% (w/w). Lower starch concentrations resulted in a broader size distribution of spherulites of more regular shape. At 30% (w/w) of starch, spherulites often impinged on one another distorting the shape, and were often observed in clusters.

3.2. Effect of starch type (amylose:amylopectin ratio)

Aqueous samples of 30% (w/w) *ae* 70 HAS, *ae* 50 HAS,

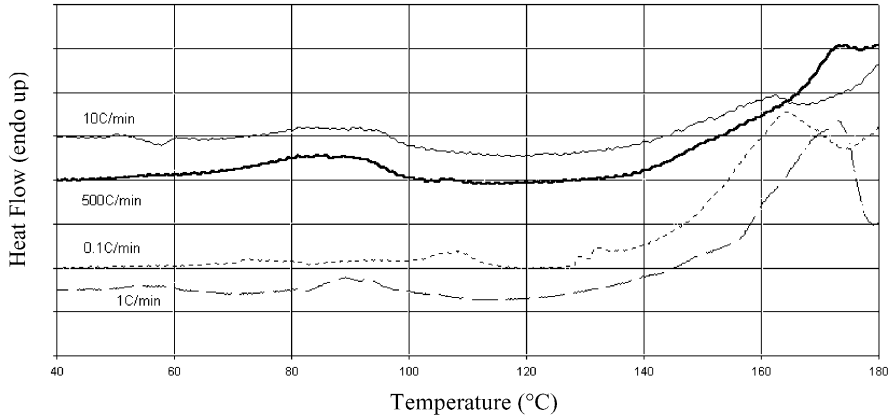

Fig. 5. Differential scanning calorimetry thermograms produced on heating (10 °C/min) previously gelatinized (180 °C) starch cooled at: (A) 0.1 °C/min, (B) 1.0 °C/min, (C) 10 °C/min, and (D) 500 °C/min, and stored for 2 days.

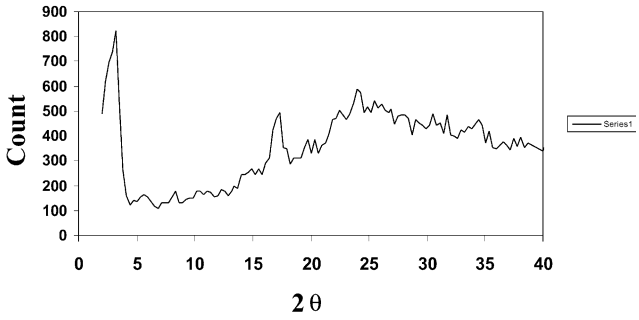

Fig. 6. X-ray diffraction patterns of spherulitic semi-crystalline starch. Scan rate 0.48°/min.

ordinary maize starch (OMS), WMS, purified amylose (from *ae* 70 HAS) and amylopectin (from waxy starch) were quenched from 180 to 10 °C at 150 °C/min. Samples were then either immediately rescanned in the DSC or observed soon after by microcopy.

Samples of *ae* 50 and 70 HAS displayed a melting endotherm with a peak temperature of 90–100 °C (Fig. 7), suggesting that spherulites had been formed. Only a very small endotherm appeared in this range for OMS and no endotherm was observed for WMS (Fig. 7). Results from light microscopy clearly substantiated these findings; spherulites were numerous in *ae* 50 and 70 HAS samples, but difficult or impossible to find in ordinary and waxy starch samples. Spherulites were easily formed in samples of amylose that had been purified from *ae* 70 HAS (Fig. 8A and B). However, the melting range extended from near 90 to ca. 140 °C with a peak temperature of 125–130 °C and slightly higher enthalpy (9–10 J/g) than those formed from the native *ae* 70 HAS (Fig. 8C). Spherulites were rarely present, and never abundant, in amylopectin samples. However, it is unclear whether these comprised contaminating amylose or were an example of amylopectin spherulites.

Assuming the 'classical' model for spherulite structure (Keller, 1968; Sharples, 1966; Sperling, 1992), one might reasonably expect amylose to fold into crystalline lamellae more easily than amylopectin. Chowdhury, Haigh, Mandelkern, and Alamo (1998) reported a decrease in melting temperature and a progressive deterioration of supermolecular structure (i.e. loss of spherulitic structure) as the concentration of branch points in ethylene–vinyl acetate copolymers was increased.

'Impurity' segregation at the growing crystalline front has been advanced as an explanation for spherulite formation (Keller, 1968). For polymers containing molecules of different molecular weight, phase separation may occur during crystallization (Keller, 1968). It is quite conceivable that immiscible droplets of amylopectin become trapped in the growing spherulite. This would all be the more probable if amylose were the continuous phase, which is to be expected at higher amylose:amylopectin ratios (Hermansson et al., 1995; Leloup et al., 1991).

Impurity segregation does not explain lamella branching. Leloup et al. (1992) have proposed a 'continuous model' for amylose gels with branch points. In this model the amylose chain axes were nearly perpendicular to the microfiber axis. Spherulites possessing this type of lamella radiating outward would appear negatively birefringent, as did those observed here. It is possible that the lightly branched 'intermediate' material of HAS is ideal for spherulite formation, having natural branch points but with long chains capable of forming lamella.

3.3. Influence of a high-temperature holding period (phase separation)

To investigate the potential influence of phase separation on the crystallization behavior, a 1 h holding period was included in the cooling ramp at 95 °C, just above the peak melting temperature. Melting behavior was observed at 1 and 7 days post-gelatinization, with and without inclusion of a hold, to investigate the long-time kinetics of crystallization. Aqueous samples of 30% (w/w) *ae* 70 HAS were first heated in the DSC to 180 °C at 10 °C/min and then either quenched to 10 °C at 150 °C/min or cooled to 95 °C at 10 °C/min and held there for 60 min before being quenched to 10 °C at 150 °C/min. Samples were stored at 20 °C for either 1 or 7 days before being scanned in the DSC to 180 °C at 10 °C/min or used for microscopy.

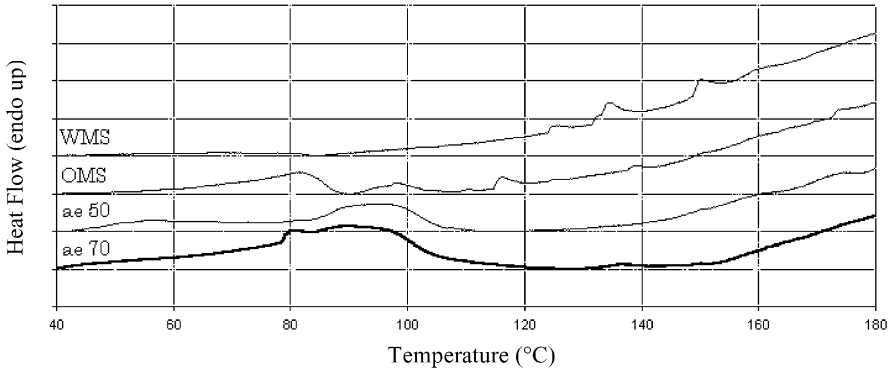

Fig. 7. Differential scanning calorimetry thermograms produced on heating (10 °C/min) previously gelatinized (180 °C) starch: (A) *ae* 70 HAS, (B) *ae* 50 HAS, (C) OMS and (D) WMS immediate rescan.

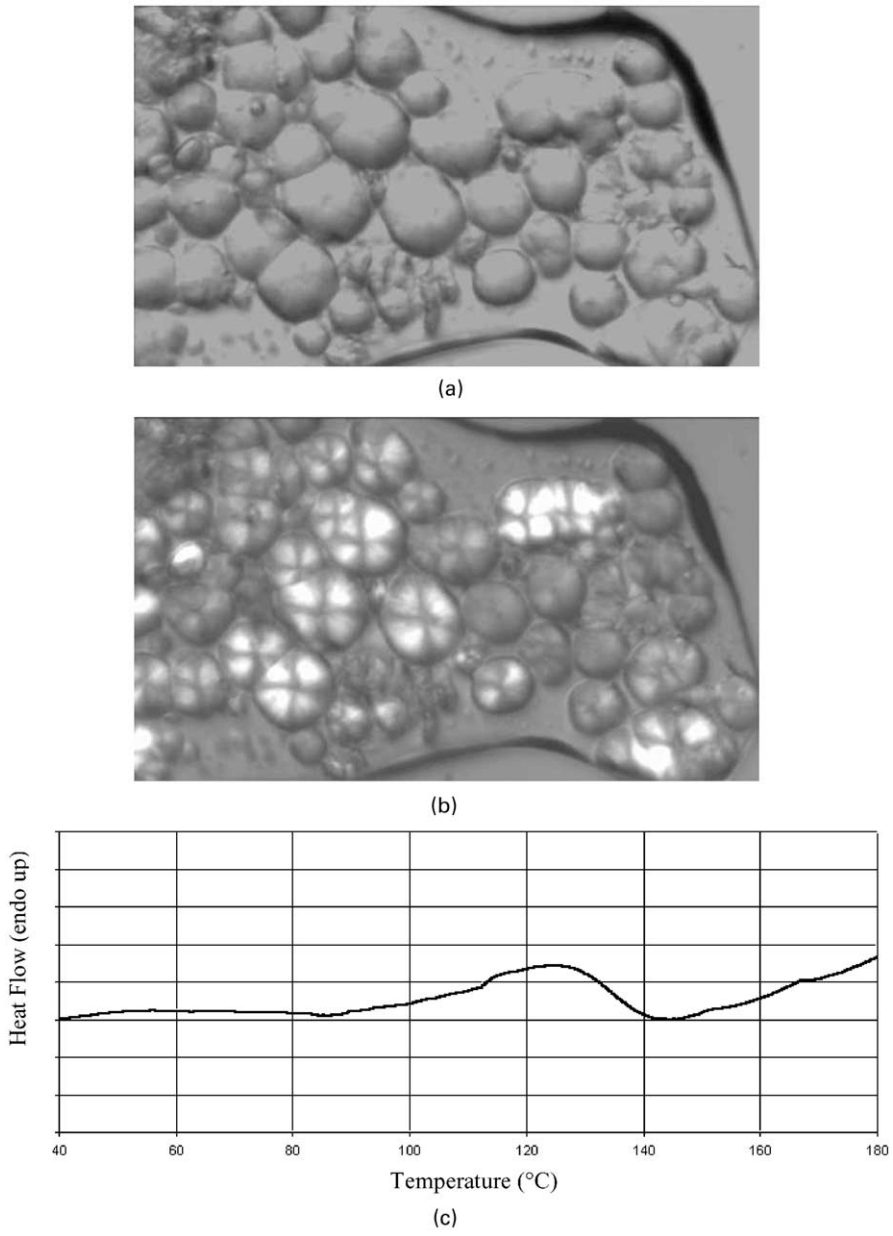

Fig. 8. Spherulites formed by amylose purified from *ae* 70 high-amylose maize starch: (A) light micrograph (image size $45 \times 80\ \mu m^2$), (B) polarized light micrograph (image size $45 \times 80\ \mu m^2$), and (C) thermogram.

With the inclusion of a holding period the thermograms became more complex (Fig. 9). The resolution of the broad endotherm observed in quenched samples into more distinct peaks argues for the possibility of phase separation between amylose and amylopectin, or the separation of spherulite melting from amylose–lipid complex melting events. The appearance of an endotherm at about 120 °C with the inclusion of a holding period may also indicate the formation of form IIa amylose–lipid complex (Biliaderis & Seneviratne, 1990). Transformations between forms of amylose–lipid complex, resulting in an increase in thermal stability as revealed by an increase in the peak melting temperature, have been described (Biliaderis, Page, Slade, & Sirret, 1985; Jovanovich & Añón, 1999). In both cases annealing samples between 90–95 °C increased T_m in the range 110–120 °C. The role of lipid is discussed in greater detail later.

A secondary, slower stage of crystallization is common in many polymer systems (Sharples, 1966). Two explanations for this phenomenon have been advanced: An increase in the amount of crystallinity, resulting from the crystallization of impurities which were rejected from the growing lamella during spherulite development; or an increase in the perfection of existing crystallites (Sharples, 1966). If amylopectin were rejected from the growing crystal lamellae only to crystallize separately at a later time, one would expect an increase in crystallinity over the 7-day storage period in the

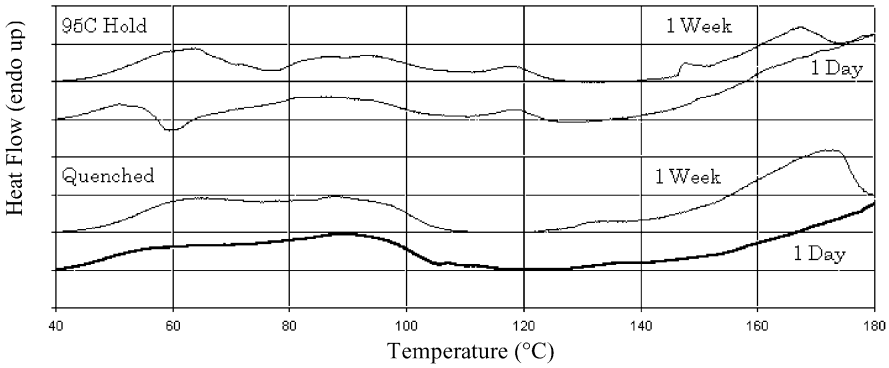

Fig. 9. DSC thermograms obtained after: (A) direct quench from 180 to 10 °C at 150 °C/min, observed after 1 day at 20 °C, (B) inclusion of a 1 h hold at 95 °C during the cooling step, observed after 1 day, (C) direct quench from 180 to 10 °C at 150 °C/min, observed after 7 days at 20 °C, and (D) inclusion of a 1 h hold at 95 °C during the cooling step, observed after 7 days at 20°C.

temperature range characteristic for amylopectin retrogradation (~60 °C). This was not unambiguously observed. Instead, a high-temperature peak (160–180 °C) often appeared in these samples. This was more notable in quenched samples and it is possible that the formation of amylose–lipid complex with the inclusion of a hold period inhibits this secondary crystallization.

In non-agitated systems, like a DSC pan, the high viscosity of the polymer melt may inhibit molecular diffusion and permit retention of some degree of chain orientation above the melting point that could then act as a template on recrystallization (Sperling, 1992). Thermal treatments that included a 1 h holding period at 95 °C, whether during the cooling ramp or during the heating ramp, produced spherulites of larger average size and of more regular shape than simple heat–quench cycles (Fig. 10). This implies some 'memory effect' where the influence of the holding period was not erased by subsequent thermal cycling. The inclusion of a holding period or repeated heat–quench cycling increased the spherulite melting point.

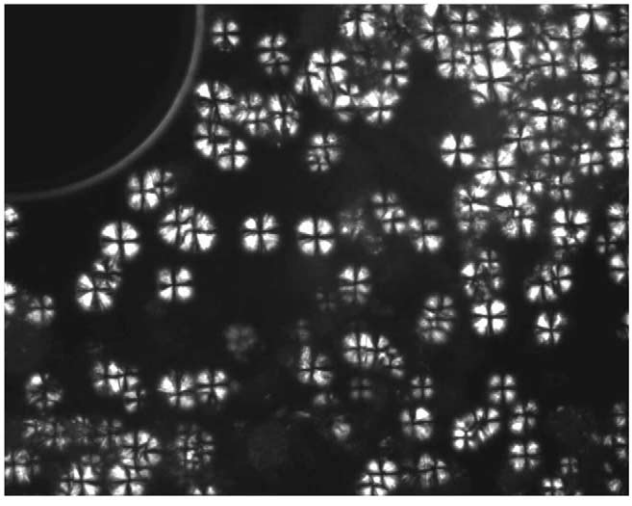

Fig. 10. Polarized light micrograph of spherulites produced from 30% (w/w) *ae* 70 HAS in water by four melt–crystallization cycles between 180 and 10 °C including a 1 h hold at 95 °C during the heating ramp of cycle 2 (image size $285 \times 360\ \mu m^2$). Compare to Fig. 1B. Heating rate 10 °C/min. Cooling rate 150 °C/min.

3.4. Effect of co-solutes

The observation of spherulites in dispersed, dried HAS (lipid-free and non-granular) and in blends of amylose and amylopectin demonstrates that starch lipids are not required for their formation and that their origin does not lie in residual granular order. No endotherm appears at 120 °C in the lipid-free DDS–HAS, supporting the conclusion that this endotherm in Fig. 9 represents amylose–lipid complex melting.

The case for phase separation is clearer in thermograms of DSS–HAS and mixtures of amylose and amylopectin (Fig. 11) than in native starches (Fig. 9). With the inclusion of a 1 h holding period at 95 °C, the broad endotherm occurring in the range 40–100 °C in the amylose–amylopectin mixture is cleanly resolved into two, with a higher temperature endotherm similar to that obtained for amylose alone (vis-à-vis Fig. 8C). For DDS–HAS, in which the amylose and amylopectin could be expected to be more intimately mixed initially, a unimodal peak became nearly bimodal with the inclusion of the hold.

Shi, Capitani, Trzasko, and Jeffcoat (1998) observed endotherms at ~95 °C on rescan of gelatinized 25% *ae* 50 and 70 HAS in water, and interpreted these as the melting of amylose–lipid complex. They noted that the melting peak of the amylose–lipid complex was 'broader and larger' in HAS when compared to normal maize starch (Shi et al., 1998). It is apparent from the present work that care must be taken in interpretation of DSC thermograms. It is possible that endotherms occurring on immediate reheating at temperatures near 100 °C could arise from spherulitic crystallinity whether or not lipid is present. There is evidence that the melting endotherms of amylose–lipid complex and spherulites overlap. The possibility that a portion of the peak observed at 90 °C is amylose–lipid complex cannot be ruled out. In fact, neither can the possibility that

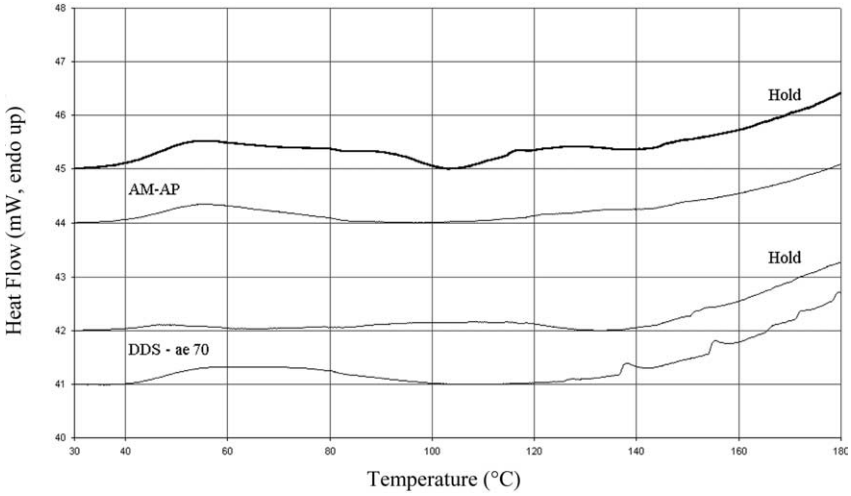

Fig. 11. DSC thermograms for dispersed, dried starch (DDS-*ae* 70) and amylose–amylopectin mixtures (AM–AP) heated to 180 °C followed by either: (A) direct quench from 180 to 10 °C at 150 °C/min, or (B) inclusion of a 1 h hold at 95°C during the cooling step (hold).

amylose–lipid complex exists within the spherulite, but it is not necessary for spherulite formation.

Granular *ae* 70 HAS was mixed into solutions of 15 and 60% (w/w) sucrose so that the total concentration of dry polymer was 10% (w/w). This mixture was heated to 180 °C at 10°C/min, followed by cooling to 10 °C at 10 °C/min. Samples were analyzed by microscopy after 1 day of storage at 20 °C.

Well-shaped, optically-active rods and occasional fuzzy clusters predominated. Any spherulites that were found were relatively small (3–10 μm), often had distorted Maltese crosses, and were of a dull appearance. Sucrose is known from ^{13}C NMR studies to interact with amylopectin to influence retrogradation kinetics (Farhat, Blanshard, Melvin, & Mitchell, 1997). One may speculate that sucrose addition leads to slower crystallization kinetics and therefore a change from spherulitic to axialitic structure. The possible role of sucrose in the development of the starch granule has recently been in focus, since it has been discovered that sucrose is the most abundant metabolite found in starch granules (Kossmann & Lloyd, 2000).

4. Conclusions

Spherulitic structure similar, but not identical, to granular starch was obtained by rapid crystallization of gelatinized native-size maize starch. Recently, Smith (1999) concluded that the organization of polymers within the granule requires primarily physical rather than biological explanations. However, there have not been any convincing reports of granule formation in vitro from either gelatinized (disordered) starch or polysaccharide mixtures, despite many attempts (Gidley & Cooke, 1991). Among the complexities of starch granule organization to be explained are differences in structure between the core and the periphery of the granule (Smith, 1999), for example, anomalous phenomena such as the 'blue cores' of some waxy-type starch granules. The size and three-dimensional morphology of the spherulites we observed were nearly identical to immature wheat starch granules 4 days after germination, see for example fig. 10.4b in Duffus (1984), and different from the spherulites of short chain amylose or cellulose previously reported (Kobayashi et al., 2000; Ring et al., 1987). Helbert et al. (1993) observed that the enzymatic digestibility of spherulites (of short chain amylose) was similar to that of the hilum of starch granules. Evans and Thompson (2001) observed different patterns of enzyme digestion in HAS vis-à-vis common corn starch. Enzymatic degradation proceeded in a radial direction in HAS granules, but tangentially in normal maize starch. We suggest that the starch polymers found in *ae* mutants are similar to those present at the early stages of granule development, and that granule organization begins with the incipient crystallization of spherulites.

Acknowledgements

We are grateful to Drs Jeffery Klucinec and Donald Thompson for kindly supplying dispersed dry starch, amylose and amylopectin samples. We are grateful to Dr Simon Gilroy, Department of Biology, Penn State University, for allowing us use of the microscopy facilities. We thank Dr Koushik Seetharaman for the thoughtful discussions.

References

Bassett, D. C. (1981). *Principles of polymer morphology*, Cambridge, UK: Cambridge University Press.

Battista, O. A. (1975). *Microcrystal polymer science*, New York: McGraw-Hill.

Biliaderis, C. G., & Seneviratne, H. D. (1990). On the supramolecular

structure and metastability of glycerol monostearate–amylose complex. *Carbohydrate Polymers*, *13* (2), 185–206.

Biliaderis, C. G., Page, C. M., Slade, L., & Sirett, R. R. (1985). Thermal behavior of amylose–lipid complexes. *Carbohydrate Polymers*, *5*, 367–389.

Cheetham, N. W. H., & Tao, L. P. (1998). Variation in crystalline type with amylose content in maize starch granules: An X-ray powder diffraction study. *Carbohydrate Polymers*, *36*, 277–284.

Cho, K. W., Li, F. K., & Choi, J. (1999). Cystallization and melting behavior of polypropylene and maleated polypropylene blends. *Polymer*, *40* (7), 1719–1729.

Chowdhury, F., Haigh, J. A., Mandelkern, L., & Alamo, R. G. (1998). The supramolecular structure of ethylene–vinyl copolymers. *Polymer Bulletin*, *41*, 463–470.

Davies, T., Miller, D. C., & Proctor, A. A. (1980). Inclusion complexes of free fatty acids with amylose. *Starch*, *5*, 149–158.

De Meuter, P., Amelrijckx, J., Rahier, H., & Van Mele, B. (1999). Isothermal crystallization of concentrated amorphous starch systems measured by modulated differential scanning calorimetry. *Journal of Polymer Science: Part B: Polymer Physics*, *37*, 2881–2892.

Duffus, C. M. (1984). Metabolism of reserve starch. In D. H. Lewis, *Storage carbohydrates in vascular distribution, physiology and metabolisim* (pp. 231–252). Cambridge, UK: Cambridge University Press Chapter 10.

Evans, A., & Thompson, D. B. (2001). Residual granule structures are observed for resistant starch. *Food Industry Conference*, Lancaster, PA, April 3.

Farhat, I. A., Blanshard, J. M. V., Melvin, J. L., & Mitchell, J. R. (1997). The effects of water and sugars upon the retrogradation of amylopectin in the region (T–T_g) between 0 and 85°C. In P. J. Frazier, P. Richmond & A. M. Donald, *Starch structure and functionality* (pp. 86–95). Cambridge, UK: The Royal Society of Chemistry.

Gidley, M. J., & Cooke, D. (1991). Aspects of the molecular organization and ultrastructure in starch granules. *Biochemical Society Transactions*, *19* (3), 551–555.

Godet, M. C., Bouchet, B., Colonna, P., Gallant, D. J., & Buleon, A. (1996). Crystalline amylose–fatty acid complexes: Morphology and crystal thickness. *Journal of Food Science*, *61* (6), 1196–1201.

Haudin, J. M. (1986). Optical studies of polymer morphology. In G. H. Meeten, *Optical properties of polymers* (pp. 167–264). London: Elsevier Chapter 4.

Helbert, W., Chanzy, H., Planchot, V., Buleon, A., & Colonna, P. (1993). Morphological and structural features of amylose spherocrystals of A-type. *International Journal of Biological Macromolecules*, *15*, 183–187.

Hermansson, A. -M., Kidman, S., & Svegmark, K. (1995). Starch—A phase-separated biopolymer system. In S. E. Harding, S. E. Hill & J. R. Mitchell, *Biopolymer mixtures* (pp. 225–245). Nottingham, UK: Nottingham University Press.

Hoover, R. (1995). Starch retrogradation. *Food Reviews International*, *11* (2), 331–346.

Jovanovich, G., & Añón, M. C. (1999). Amylose–lipid complex dissociation. A study of the kinetic parameters. *Biopolymers*, *49*, 81–89.

Kalichevsky, M. T., & Ring, S. G. (1987). Incompatibility of amylose and amylopectin in aqueous solution. *Carbohydrate Research*, *162*, 323–328.

Keller, A. (1968). Polymer crystals. *Reports on Progress in Physics*, vol. XXXI, Part II, pp. 623–704.

Klucinec, J. D. (1997). *The composition and physical behavior of selected high-amylose maize starches and of fractions determined by differential alcohol precipitation*. M.S. Thesis, The Pennsylvania State University, pp. 60–61.

Klucinec, J. D., & Thompson, D. T. (1996). Fractionation of high-amylose maize starches by differential alcohol precipitation and chromatography of the fractions. *Cereal Chemistry*, *75*, 887–896.

Kobayashi, S., Hobson, L. J., Sakamoto, J., Kimura, S., Sugiyama, J., Imai, T., & Itoh, T. (2000). Formation and structure of artificial cellulose spherulites via enzymatic polymersization. *Biomacromolecules*, *1* (2), 168–173.

Kossmann, J., & Lloyd, J. (2000). Understanding and influencing starch biochemistry. *Critical Reviews in Plant Sciences*, *19* (3), 171–226.

Leloup, V. M., Colonna, P., & Buleon, A. (1991). Influence of amylose–amylopectin ratio on gel properties. *Journal of Cereal Science*, *13*, 1–13.

Leloup, V. M., Colonna, P., Ring, S. G., Roberts, K., & Wells, B. (1992). Microstructure of amylose gels. *Carbohydrate Polymers*, *18*, 189–197.

Maxfield, J., & Mandelkern, L. (1977). Crystallinity, supermolecular structure, and thermodynamic properties of linear polyethylene fractions. *Macromolecules*, *10* (5), 1141–1153.

Moates, G. K., Noel, T. R., Parker, R., & Ring, S. G. (1997). The effect of chain length and solvent interactions on the dissolution of the B-type crystalline polymorph of amylose in water. *Carbohydrate Research*, *298*, 327–348.

Richardson, P. H., Jeffcoat, R. & Shi, Y. -C. (2000). High-amylose starches: From biosynthesis to their use as food ingredients. *MRS Bulletin, December*, pp. 20–24.

Ring, S. G., Miles, M. J., Morris, V. J., Turner, R., & Colonna, P. (1987). Spherulitic crystallization of short chain amylose. *International Journal of Biological Macromolecules*, *9*, 158–160.

Sandstedt, R. M. (1965). Fifty years of progress in starch chemistry. *Cereal Science Today*, *10*, 305–314 (see also pp. 358–359).

Sharples, A. (1966). *Introduction to polymer crystallization*, New York: St. Martins Press.

Shi, Y. C., Capitani, T., Trzasko, P., & Jeffcoat, R. (1998). Molecular structure of a low-amylopectin starch and other high-amylose maize starches. *Journal of Cereal Science*, *27*, 289–299.

Smith, A. (1999). Making starch. *Current Opinion in Plant Biology*, *2*, 223–229.

Sperling, L. H. (1992). The crystalline state. *Introduction to physical polymer science* (2nd ed). (pp. 198–278). New York: Wiley Chapter 6.

Takeda, Y., Hizukuri, S., & Juliano, B. O. (1986). Purification and structure of amylose from starch. *Carbohydrate Research*, *148*, 299–308.

Yuryev, V. P., Nemirovskaya, I. E., & Maslova, T. D. (1995). Phase state of starch gels at different water contents. *Carbohydrate Polymers*, *26*, 43–46.